Molecular dynamics simulations of the ionic liquid-borophene interface

Víctor Gómez-González[a,1], J. Manuel Otero-Mato[a,1], Hadrián Montes-Campos[a], Xabier García-Andrade[a], Amador García-Fuente[b], Andrés Vega[c], Jesús Carrete[d], Oscar Cabeza[e], Luis J. Gallego[a], Luis M. Varela[a,*]

[a] *Grupo de Nanomateriales, Fotónica y Materia Blanda, Departamento de Física de Partículas, Facultade de Física, Universidade de Santiago de Compostela, Campus Vida s/n, E-15782 Santiago de Compostela, Spain*
[b] *Departamento de Física, Universidad de Oviedo, E-33007 Oviedo, Spain*
[c] *Departamento de Física Teórica, Atómica y Óptica, Universidad de Valladolid, E-47011 Valladolid, Spain*
[d] *Institute of Materials Chemistry, TU Wien, A-1060 Vienna, Austria*
[e] *Departamento de Física y Ciencias de la Tierra, Facultade de Ciencias, Universidade da Coruña, Campus A Zapateira s/n, E-15071 A Coruña, Spain*

Abstract

In this work we perform molecular dynamics simulations of mixtures of a prototypical protic ionic liquid, 1-butyl-3-methylimidazolium tetrafluoroborate ([BMIM][BF_4]), with lithium tetrafluoroborate ($LiBF_4$), confined between two borophene walls of three different surface charges, -1, 0 and +1 e/nm^2, where e is the elementary charge. The properties of the system are analyzed by means of ionic density profiles, angular orientations of $[BMIM]^+$ cations close to the wall and vibrational densities of states for the salt cations close to the walls. Lateral structure of the first layer close to the surface is also studied on one hand, calculating Minkowski parameters and the Shannon entropy of the patterns of the 2D density maps of the anions placed there and, on the other hand, computing the 2D-Fourier transform of the positions of these anions. Our results are compared with those obtained previously for the same mixtures confined between two graphene walls. Although similarities exist between both cases, interesting differences are observed in the lateral structure that the ionic liquid

*Corresponding author
Email address: luismiguel.varela@usc.es (Luis M. Varela)
[1] Contributed equally to this work.

adopts near borophene interfaces due to their strong anisotropy. Particularly, we have observed that borophene induces more markedly ordered 2D patterns in the innermost layer of the ionic liquid electric double layer, specially when they are charged. It is this feature what makes borophene a potential candidate to battery electrode applications with possibilities beyond those of graphene.

---

1. Introduction

The interest in ionic liquids (ILs) has been constantly increasing during the past twenty years, mainly because of their large number of their potential applications [1, 2]. Indeed, experimental, theoretical and computer simulation studies have been performed for the study of these sometimes called "designer solvents" [3], as this is one of their most interesting properties. Another one is their wide electrochemical window, which makes them very promising for applications in electrochemical devices such as batteries, supercapacitors or fuel cells [4–7], even when the addition of some electroactive species to the solvent is necessary in many of these applications [8–10].

A great number of publications centered around this particular topic have been reported, dealing with alkali metals combined with various ILs (mainly bis(trifluoromethylsulfonyl)imide, TFSI, as the anion, and cations belonging to the pyrrolidinium, piperidinium, alkylammonium or imidazolium families) [11–34], but also with some higher-valence salts [35–43]. Some of these studies have been done using computer simulation, including classical molecular dynamics (MD) and density functional theory (DFT), to analyze the microscopic mechanisms behind solvation, structure, and transport in these media, both in the bulk or at the electrochemical interface, usually represented by a graphene virtual electrode (see, e. g., Refs. 44 and 45). The ordering of IL-based electrolytes at this electrochemical interface has been studied with great detail for mixtures of ILs with Li [41, 42, 46, 47], Mg [41, 42], and Al [43].

Many other single-layer or few-layer 2D materials have already been synthesized or predicted whose role has not been explored yet for these types of

studies (see, e. g., Ref. 48 and those cited therein). A 2D nanostructure that has recently attracted a great deal of attention is borophene, whose existence was theoretically predicted some time ago [49], but whose experimental realization in the form of sheets on a Ag(111) substrate was reported only recently by Mannix *et al.* [50]. Borophene exhibits structural anisotropy and polymorphism, which results in a range of properties unique to 2D materials, including a combination of metallicity, mechanical flexibility, transparency and superconductivity [51].

Early DFT calculations suggested that single-atomic-layer boron sheets composed of triangular and hexagonal motifs were locally stable, the more stable structure of this kind being called the α sheet [52]. However, subsequent research predicted two novel 2D boron phases with nonzero thickness that are considerably more stable than the α sheet [53]. One of these phases shows a Dirac cone in its electronic band structure, which renders it especially interesting from electronic perspectives. It has a buckled structure containing 8 atoms in the unit cell, being considerably more complex than other 2D materials such as graphene; it will be henceforth referred to as the Pmmn8 phase, or simply the β sheet. The structure of the boron monolayer obtained by Mannix *et al.* on the Ag(111) substrate has Pmmn symmetry with lattice constants a and b equal to 2.89 Å and 5.00 Å, respectively [50]. However, free standing relaxation of this structure removes the slight corrugation along the a direction, preserving the buckling along the b direction [50]. The resulting Pmmn structure of the freestanding borophene has 2 boron atoms per unit cell and lattice constants $a = 2.865$ Å and $b = 1.67$ Å; this structure will be denoted as the Pmmn2 or γ phase.

Recent calculations of the phonon spectra of the β and γ phases have shown than both of them are mechanically stable [54, 55]. However, the phonon spectra of the γ phase presents a low-frequency valley in the ZA branch between γ and X, suggesting that the energetic cost of inducing a transition to the β phase is small. By contrast, the β phase has not corresponding soft modes, and it is thus a better candidate for mechanical stability in practice. Experimental measurements and theoretical calculations show that both supported and free-

standing Pmmn2 borophene are highly anisotropic 2D metals [50]. On the other hand, the β phase of borophene has been predicted to have a rather large thermal conductivity comparable to that of MoS_2, and a significant in plane anisotropy comparable in order of magnitude with that of black phosphorene [54].

Recent studies have investigated possible practical applications of the α, β and γ phases of borophene; for instance, for hydrogen storage after appropriate decoration of these sheets with Li atoms [56–58]. However, a potential application of borophene, not explored in detail yet (although some works about this topic have been reported [59]), is its possible use as a battery electrode. For that, one very important aspect is a detailed knowledge of the actual effect of a borophene layer on the structure of the electrolyte, and this is precisely the main goal of this article.

In the present paper, we analyze the behaviour of both the pure aprotic IL [BMIM][BF_4] and its mixture with $LiBF_4$ confined near two borophene sheets in the most stable of its phases (the β or Pmmn8 sheet), something that, to our knowledge, has not been performed yet. We also study the differences that exist between the behaviors of IL + borophene systems and those of the IL + graphene systems that were reported in Refs. 41 and 46 (some additional calculations for the latter system are performed for this paper), as these differences could give us very relevant information regarding the future applications of IL+borophene systems in real electrochemical devices. As we will see in this paper, the main difference with graphene is that much more ordered spatial patterns are in the innermost layer of the electric double layer, induced by the borophene wall, and the nontrivial fact that charging the walls leads to more ordered configurations than neutral walls, contrary to what seems to happen at the graphene-based electrochemical interface. It is this feature what makes borophene a promising candidate for battery electrode applications, with yet unexplored possibilities potentially beyond those of graphene.

The remainder of this paper is structured as follows: simulation details are explained in section 2, our results are presented and discussed in section 3, and finally, in section 4, we summarize our main conclusions.

2. Computational details

The borophene sheet used in the MD simulations of this paper was constructed using the DFT package VASP [60–63] with projector-augmented-wave datasets and the Perdew-Burke-Ernzerhoff approximation to exchange and correlation. A sheet of 8 boron atoms, corresponding to the unit cell of a Pmmn8 borophene sheet (see Fig. 1), was simulated setting the total number of electrons in the systems to 24.148, 24 and 23.853, which correspond to macroscopic walls of surface charge densities of -1, 0 and +1 e/nm^2, respectively, where e is the elementary charge. The z dimension was set to 20 Å, in order to have sufficient vacuum so as to avoid influence from periodic replicas. Monkhorst-Pack grids of $20 \times 20 \times 1$ were employed for the calculations. The partial charges of each atom in the unit cell were calculated from the corresponding charge density using the Bader method [64–67]. Those partial charges were used for the MD parametrization of a borophene sheet of size 6.33×6.51 nm^2, which was built by replicating the elemental DFT-calculated unit cell.

MD simulations reported in this paper were carried out by means of the GROMACS package (version 2019) [68, 69], using the OPLS-AA force field developed by Jorgensen [70] for diverse organic liquids, in order to parametrize the simulated atoms. The MD simulation procedure for the confined system can be found in Ref. 42. All simulations are carried out at room temperature, $T = 298.15$ K. Only calculations for pure IL and lithium salt molar concentration of 10% were performed.

3. Results and discussion

In this section we report the results for all calculated quantities in the systems confined between borophene walls, as well as their comparison with the analogous ones between graphene walls calculated in Refs. 46 and 71. These include density profiles for all species in the mixtures, lateral structure of the first layer closest to the walls (as well as their Minkowski parameters [72] and Shannon entropies), structural description of the adsorbed layers using 2D-Fourier

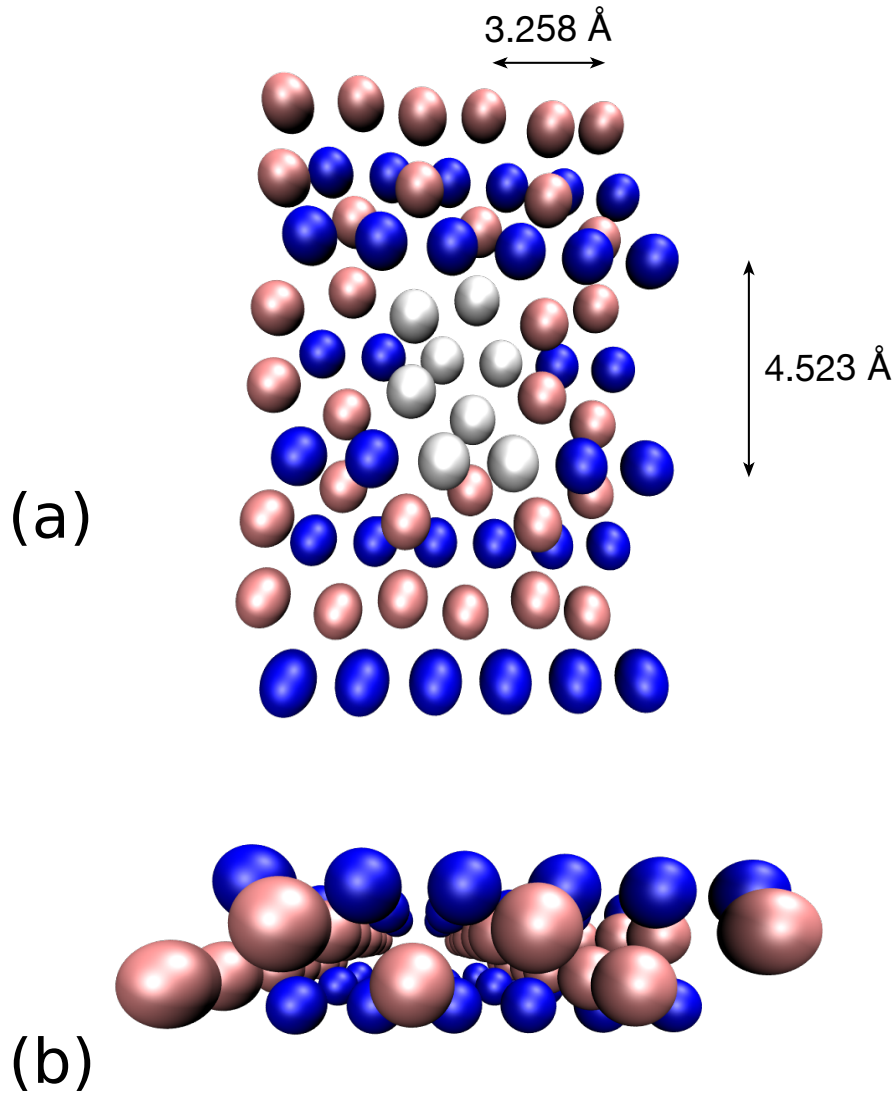

Figure 1: Top (a) and side (b) views of the β (Pmmn8) sheet of boron. The unit cell is colored in white in (a), while the two populations of boron atoms with different charges of the sheet are colored in pink and blue. Annotated distances correspond to the separation between atom lines with the same partial charge.

transforms, angular orientations of IL cations, a comparison between the closest distance of the lithium salt cation to graphene and borophene walls and the vibrational density of states (vDOS) of the salt cation in the mixtures, both in the bulk and near the interface.

The comparison between number densities near the borophene interfaces of pure IL and those of its mixtures with lithium salt is shown in Fig. 2. It has to be mentioned that the results for systems between graphene walls, which are used for comparison and are also shown in Fig. 2, are those reported in Refs. 41 and 46. The most relevant result is that the addition of salt to the neat IL does not affect in a significant way the structure of the closest layers to the borophene wall, no matter its surface charge (Fig. 2 bottom). This phenomenon matches the already well-known resiliency of IL structure upon salt doping, which has been reported in previous works [41–43, 71]. There are, however, some small differences in the structure of the electric double layer when lithium cations are added, especially in the neutral interface, where the presence of Li^+ ions at 0.65 nm (Fig. 2 (b2)) induces an approach of IL anions of the second shell to the wall so they can adequately solvate the former. This effect also appears in the positively charged wall, where a shell composed of lithium cations at 0.65 nm brings additional IL anions closer to the interface.

As it is shown in Fig. 2 (bottom), the structure near the borophene interfaces of doped and neat IL is very similar, so we decided to focus on the results provided by the mixtures of IL with lithium salt. These results reveal a great degree of similarity between the structure of the electric double layer near both kinds of surfaces, with the only important difference being that all species are closer to borophene than to graphene (more details on the particular characteristics of the number densities of all species near the graphene interfaces can be found in Ref. 46).

The most novel and significant effect of the borophene walls is shown in Fig. 3, where the lateral structure of the mixtures is shown. This distribution has been calculated for a 3D slab close to the different surfaces and gives the regions in the XY plane with the highest number density of the corresponding

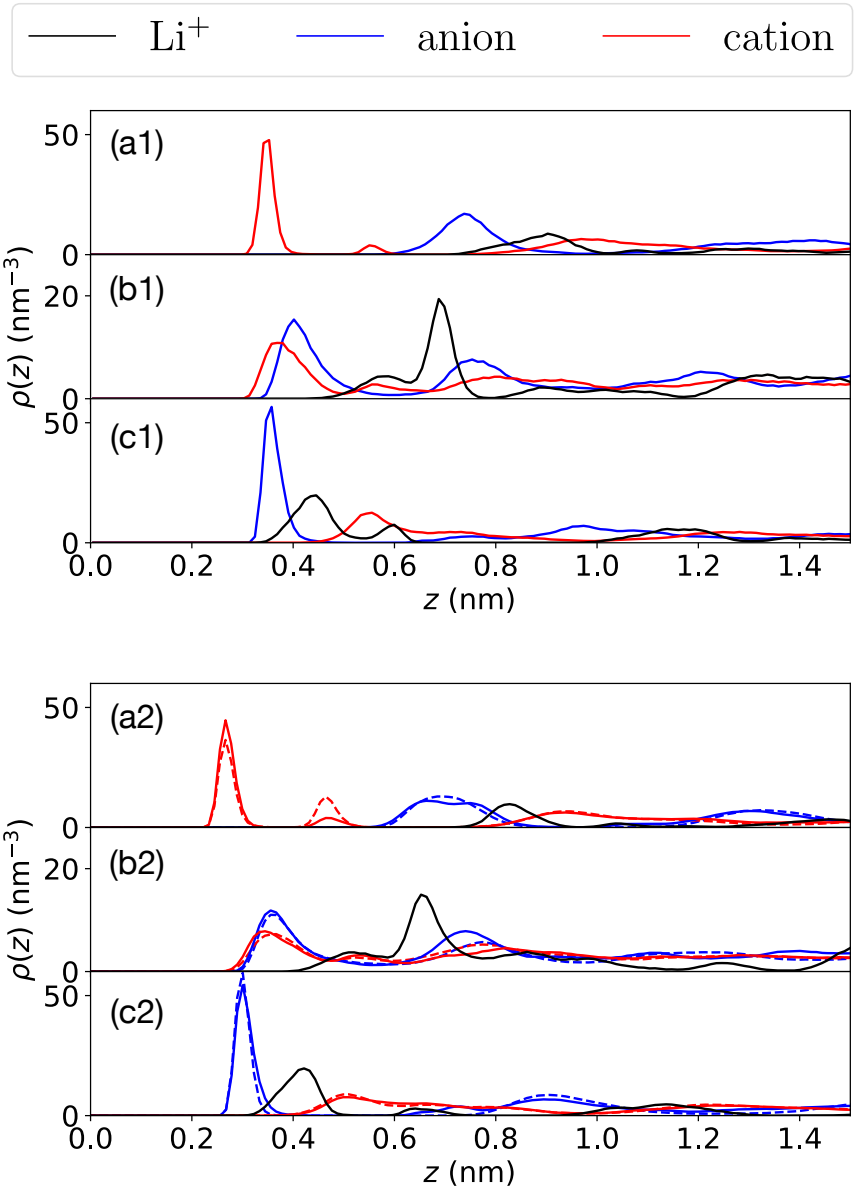

Figure 2: Number densities, $\rho(z)$, for simulated $LiBF_4$+[BMIM][BF_4] mixtures (10% molar fraction of salt). Label 1, above, corresponds to systems confined between graphene walls while label 2, below, corresponds to systems confined between borophene walls. For the last, density profiles for pure [BMIM][BF_4] simulations are also represented with dashed lines. (a) Negative wall, (b) neutral wall and (c) positively charged wall. For the sake of clarity, densities for the salt cation have been multiplied by 5 in all cases. z is the distance to the wall.

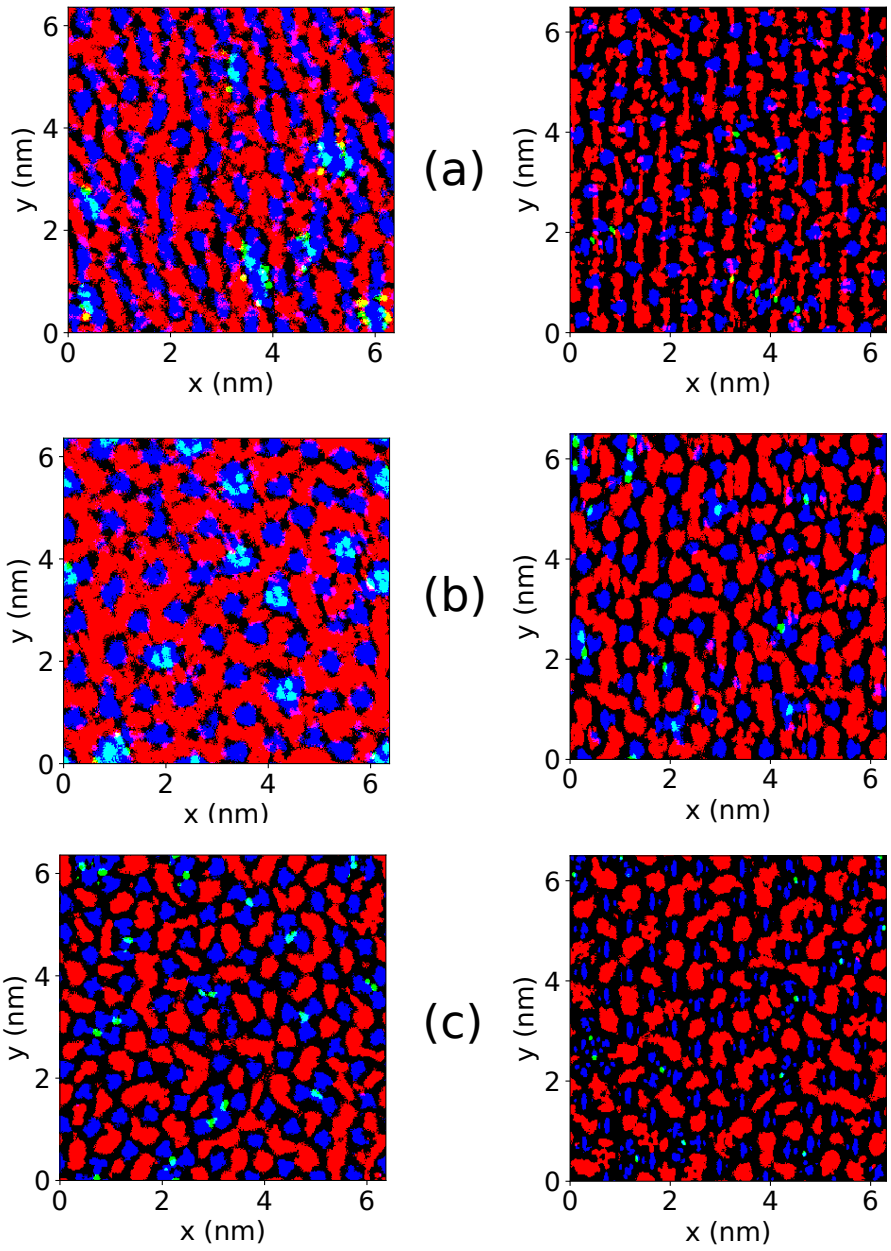

Figure 3: Comparison of lateral structure for $LiBF_4$+[BMIM][BF_4] near graphene (left) and borophene (right) walls of different surface charges: (a) negative, (b) neutral, (c) positive. $[BMIM]^+$: red, $[BF_4]^-$: blue, Li^+: green.

species, averaged in the z-direction of this slab. The thickness of the slab, d, was chosen in order to guarantee that it contains at least one entity of each of the different species in the mixture. Moreover, in order to transform these 2D-density profiles into bimodal distributions to discriminate the regions with high and low probability if ionic presence, a cutoff number density was calculated using the Otsu algorithm [73], in order to establish a mathematical consistent one for all cases.

The results for the lateral structure show that the main difference between graphene and borophene interfaces is the charge distribution at the wall. While in a graphene sheet the ionic positions are less restricted, in a borophene sheet there are two distinct layers of charge [74]. In each of those, charges are oriented in "lines of charge" (see Fig. 1), as can be clearly seen in the positively and negatively charged borophene interfaces of Fig. 3, where anions and cations are placed along vertical lines which correspond to those formed by the outermost atoms at the wall. Indeed, that causes a great change of the lateral structure with respect to the graphene wall, which is now more oriented, especially when the interface is not neutral. However, in all cases lithium cations go to the polar nanoregions of the IL, where they are solvated by IL anions forming solvation complexes [42, 43].

System	CV	MCS (Å^2)	H
graphene (-)	32%	19.7	6.23
borophene (-)	14%	6.6	4.83
graphene (0)	30%	19.6	6.18
borophene (0)	17%	8.7	5.60
graphene (+)	20%	9.9	6.25
borophene (+)	8%	2.7	4.48

Table 1: Comparison of Minkowski cluster parameters, Coverage Factor (CV) and Mean Cluster Size (MCS), as well as Shannon entropy (H), calculated for BF_4^- anions density maps in $LiBF_4$+[BMIM][BF_4] near graphene and borophene walls for different surface charges: negative (-), neutral (0) and positive (+).

Although the previous approach gives us some interesting qualitative information about the structure of the electric double layer, it is also worth to get

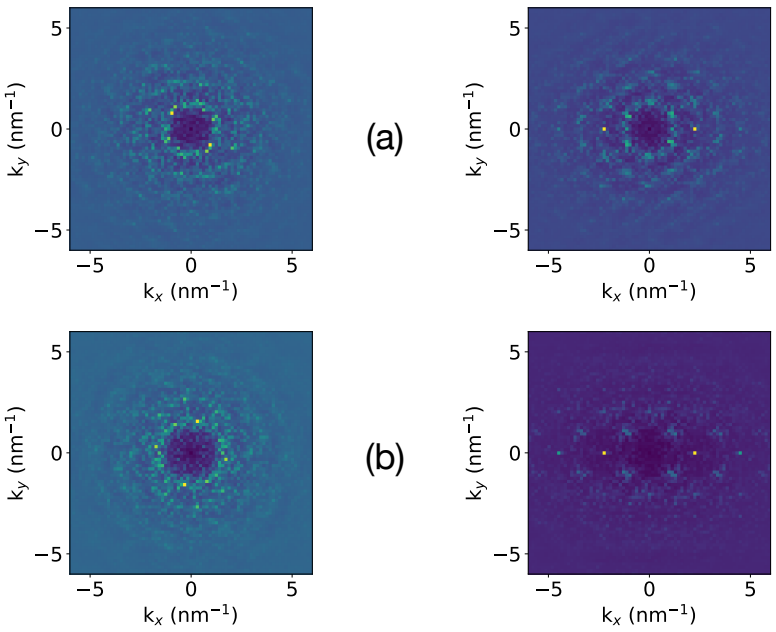

Figure 4: Comparison of time-averaged 2D-Fourier transforms of the anion positions in $LiBF_4$+[BMIM][BF_4] near graphene (left) and borophene (right) walls of different surface charges: (a) neutral, (b) positive.

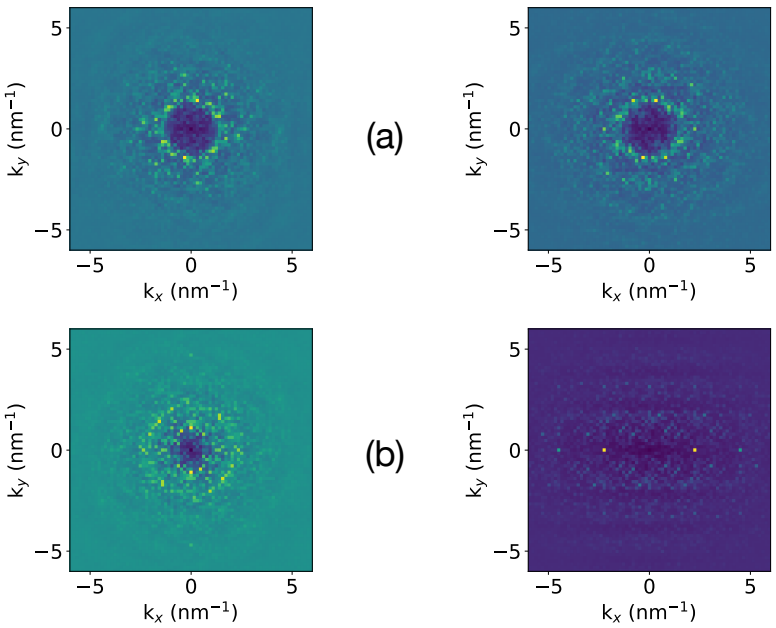

Figure 5: Comparison of time-averaged 2D-Fourier transforms of the (a) anion and (b) cation positions in $LiBF_4$+[BMIM][BF_4] near graphene (left) and borophene (right) walls of negative surface charge.

some quantitative insight. For that, we use some of the Minkowski functionals [72] in order to quantify the differences between the lateral structure of anions in both kinds of surfaces. Another important parameter which can be calculated is the Shannon entropy [75] of the 2D lateral distributions shown in Fig. 3 (before applying the cutoff), $H = -\sum_i p_i \log p_i$, where p_i is the probability of having a given intensity value in the lateral density map. This quantity gives us a way to characterize the ordering of the patterns formed by the anions positions distribution near the electrochemical interface.

The results for the mean size of the anion clusters (i.e. well defined regions where one or more anions were throughout the simulation time), the coverage factor of the wall and Shannon entropy are shown in Table 1. There we can see that there are important qualitative differences in the effect of both types of surfaces on the anion lateral ordering. In particular, it seems that borophene interfaces reduce the size of the anion clusters relative to graphene, which now have a less diffuse structure (more ordered pattern, as shown by their lower H value) imposed by the strong charge orientation in the borophene wall. This effect is less important in the neutral walls, as the charge difference between the innermost and outermost layers of borophene in that case is less important. Moreover, Shannon entropy results decrease from 5.60 (neutral) to 4.83/4.48 (negative/positive) in borophene and increase from 6.18 (neutral) to 6.23/6.25 (negative/positive) in graphene. This indicates that charging borophene generates even more ordered anion patterns, a fact with potentially far reaching consequences in their applications. On the other hand, graphene does not show the same clear trend upon charging.

Although these parameters are very useful in the characterization of these lateral density maps, it is important to remember that they are very influenced by the dynamics of the simulated species, which are not precisely reproduced with a nonpolarizable force field, such as the one used in this article [76–78]. Moreover, it has been reported that in 3D the simulated diffusion coefficients may be affected by the size and shape of the simulation box due to hydrodynamic effects [79–82]. This phenomenon was also reported by Simonnin *et al.* for

simulations of a Lennard-Jones fluid under confinement conditions but, up to our knowledge, this study has not been applied for dense ionic systems and is something which is now under study. So, in order to achieve a more precise and non-dynamic dependent description of the IL lateral structure near the interface, we calculate the time-averaged 2D-Fourier transforms of the positions of the IL cations and anions in the first layer near the walls. The results for these calculations, using the positions of the central boron for anions and the methyl-bonded nytrogen for cations, are shown in Figs. 4 and 5.

The Fourier transforms clearly show that the neutral and positively charged borophene walls induce more order than graphene ones (Fig. 4), as borophene results show more narrowed distributions in k values, while in graphene this distribution is much more homogeneous. In fact, the spatial frequencies ($\tilde{\nu}$) associated to the highest values of the distribution (represented in yellow) correspond to distances in the real space ($r = \tilde{\nu}^{-1}$) which match the characteristic distances of the borophene sheet (see Fig. 1). This means that the borophene atomic structure is partially reflected in the first ionic layer which is not the case for graphene interfaces. Regarding the negatively charged interfaces (Fig. 5), we can conclude that the lateral structure of the anions, which are in the second ionic layer, are not influenced by the wall topology and composition since rotationally symetric Fourier transform are observed (Fig. 4 (a)). However, cations in the first layer follow the same trends as anions near the positively charged wall. In summary, we can conclude that borophene interfaces induce more ordered IL lateral structures than graphene ones.

In order to analyze further the electric double layer near the borophene surface, we have also studied the orientation of IL cations closer to the wall than 1 nm. This was done by taking θ as the angle between the vector normal to the walls (parallel to the z-axis) and a vector normal to the imidazolium ring, and calculating the probability distribution functions for ring orientations as a function of $\cos(\theta)$ and/or the distance to the wall, z, which are shown in Figs. 6 and 7, respectively. Results for positive wall have not been calculated in this paper due to their lack of statistics, as near the positively charged wall there is

a low probability of presence of IL cations, so no reliable conclusions from those calculations could be obtained.

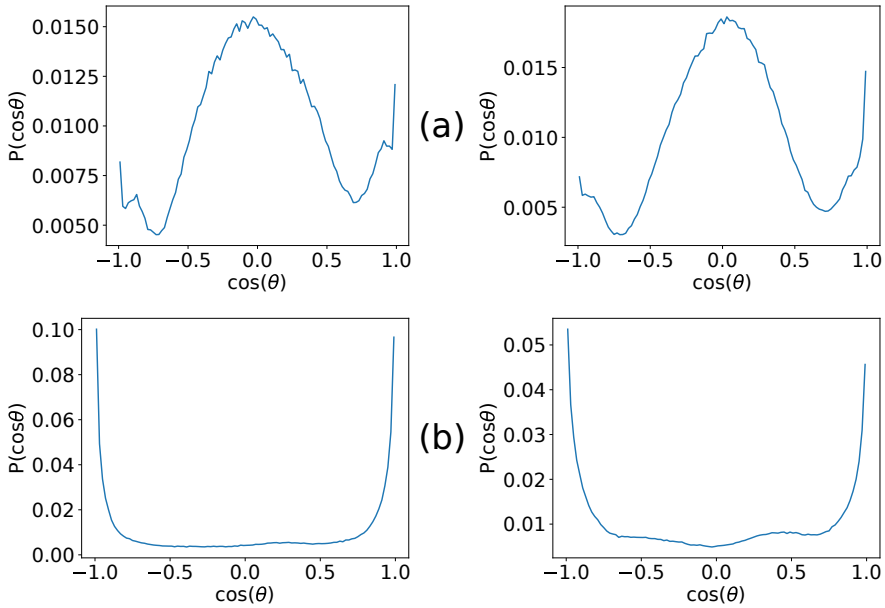

Figure 6: Orientational probability density functions for the IL cations in the first layer, $P(cos(\theta))$, for $LiBF_4$+[BMIM][BF_4] near graphene (left) and borophene (right) walls of different surface charges: (a) negative, (b) neutral.

Again, the results for graphene and borophene walls are very similar. It seems that the type of wall does not appreciably change how the IL cations are placed in the electric double layer, but it does affect the total surface charge. In fact, in both neutral graphene and borophene surfaces IL cations are mostly with the ring plane parallel to the wall, while when the wall is negatively charged the populations oriented in this way decrease and the ring is more frequently placed perpendicular to the wall, but with a large probability for angles higher than $\sim 70°$.

The shortest average distance to the surface of lithium cations in the simulations is calculated and shown for both surfaces in Fig. 8, as in a real battery containing a borophene or graphene electrode the salt cations should be able to approach enough to allow the redox reactions necessary for the operation of the

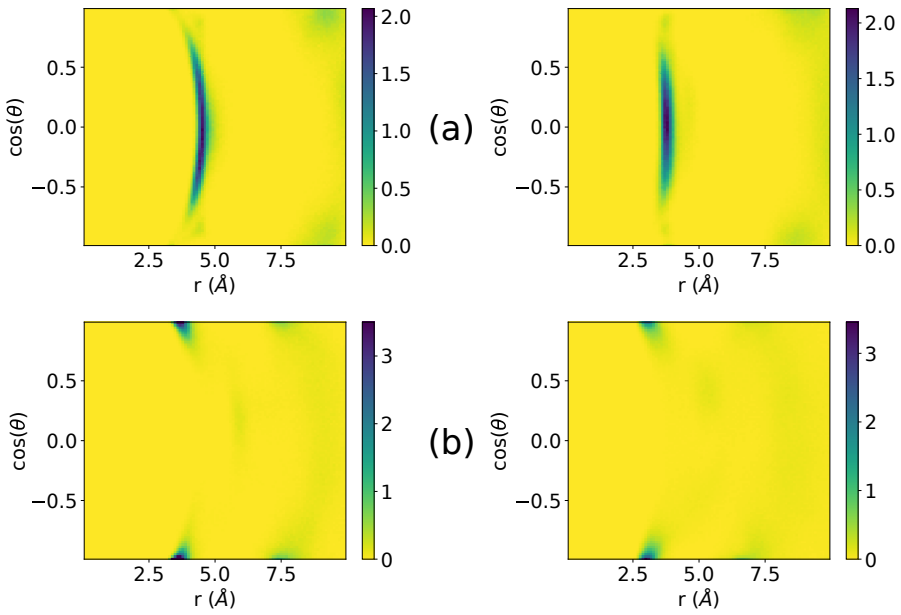

Figure 7: Orientational probability density functions as a function of $cos(\theta)$ and the z distance to the wall for the IL cations in the first layer, $P(cos(z,\theta))$, for $LiBF_4$+[BMIM][BF_4] near graphene (left) and borophene (right) walls of different surface charges: (a) negative, (b) neutral.

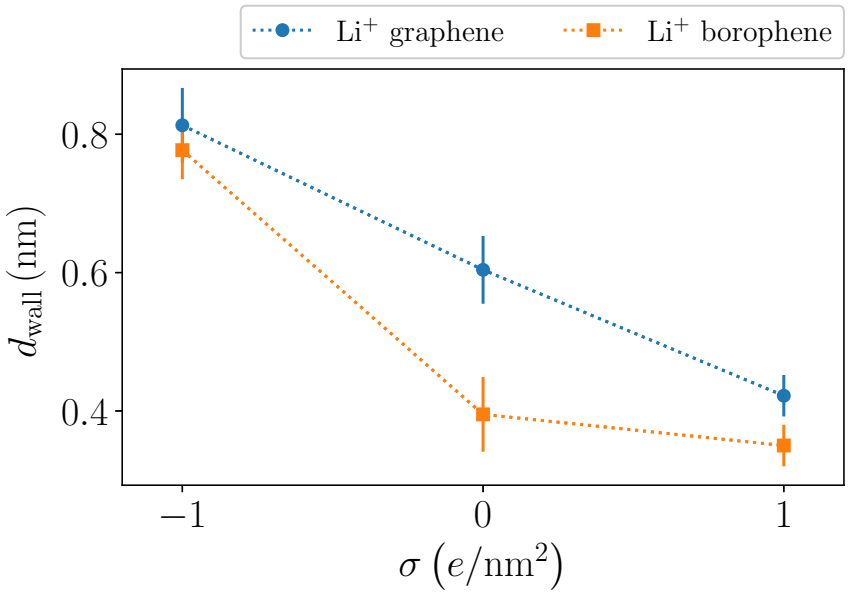

Figure 8: Average distance of closest approach to the wall of salt cations, for all the wall charges and surfaces considered in this paper. Dashed lines are guides to the eye.

battery. This comparison shows approximately the same tendencies, where Li^+ can reach closer distances to the positively charged wall than to the negatively charged one, due to the salt cation-anion complexes that form, as indicated in previous articles [41, 43]. The only difference is that lithium cations can get slightly closer to borophene walls than to graphene walls, except in neutral walls, where this difference is higher. This might be due to the higher distortion of the complexes near the neutral borophene wall, as we explain in more detail below.

We have also analyzed the single-particle dynamics of the salt cation in the mixture near both walls by means of the vibrational densities of states (vDOS) of this species near the interfaces, i.e. at distances smaller than those of the first minimum in the corresponding number densities. For this purpose, ions that met this condition were located and their average velocity autocorrelation function, $C(t)$, was calculated as

$$C(t) = \frac{\langle \vec{v}(0) \cdot \vec{v}(t) \rangle}{\langle \vec{v}(0) \cdot \vec{v}(0) \rangle} \,. \tag{1}$$

The vDOS is then simply calculated as the Fourier transform of $C(t)$. The results for lithium ions in their corresponding mixtures, both in bulk and near both graphene and borophene surfaces of variable surface charges, are shown in Fig. 9. In bulk mixtures there are three vibrational modes that correspond to oscillations of the lithium ion in its molecular cage, i.e. they depend on the kind of complexes that form. As these vDOS are very similar in bulk and near all the interfaces, we can state that salt cation-anion complexes are similar in both cases. The most important difference appears in the neutral borophene electrode, where the second and third modes are much more damped or very deformed (blue-shift of the latter with respect to the bulk one), which might indicate that salt cation complexes near this wall are weaker or different enough from the bulk and therefore allow the salt cation to reach closer distances to it than in graphene (as shown in Fig. 8), where the three modes are more similar than those in bulk.

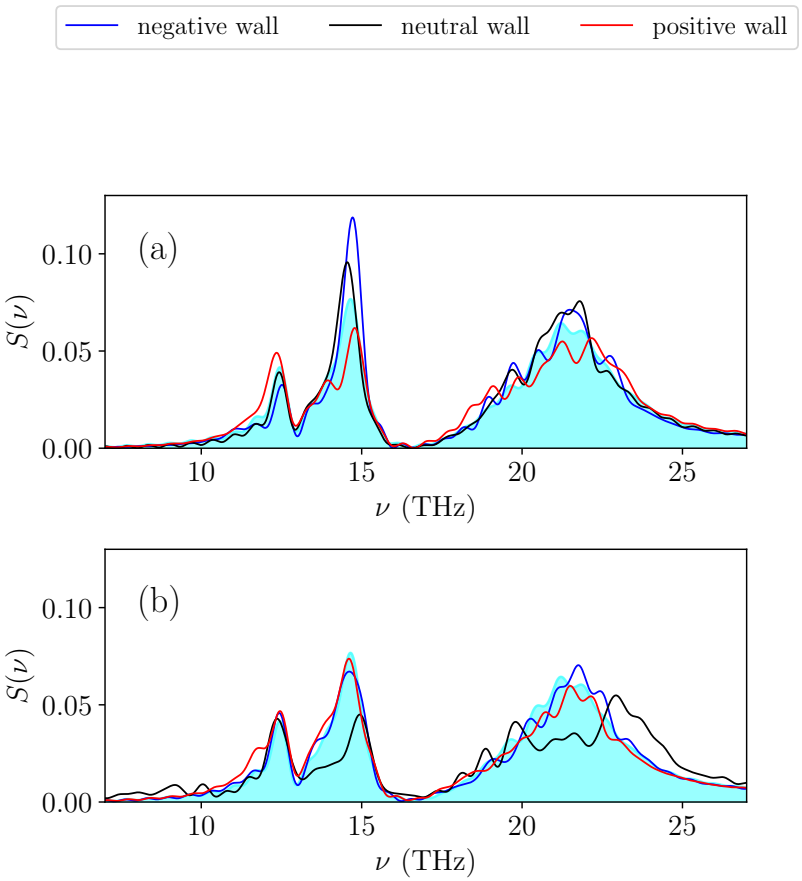

Figure 9: vDOS comparison of lithium salt cations in bulk (shaded in blue) and near a graphene wall (a) or borophene wall (b).

4. Conclusions

In this work, we perform a comparison between the effect of graphene and borophene interfaces on the structure of both pure IL, [BMIM][BF_4], and of its mixtures with $LiBF_4$, focusing on future applications of this novel 2D material in battery electrodes. Our results show that there are a lot of similarities between both systems, which might mean that borophene is at least as good electrode as graphene. However, lithium salt cations were seen to reach closer distances to the borophene electrode than to the graphene one. This might be caused by a more significant modification of the salt cation-anion complexes that form in the mixtures near the walls.

The other main (and maybe even more important) difference between graphene and borophene-based systems is the degree of ordering of the lateral structure of the IL-based mixtures near the surfaces, as in the latter there is a much more marked one (specially when it is charged), caused by the peculiarities of the structure of borophene and its charge distribution anisotropies. This might confer borophene an IL-tuning ability consistently larger than that of graphene, which might consequently provide several unexpected applications, particularly enhancing the electrochemical capabilities of this material.

5. Conflicts of interest

There are no conflicts to declare.

6. Acknowledgements

The financial support of the Spanish Ministry of Economy and Competitiveness (Projects MAT2017-89239-C2-1-P, MAT2017-89239-C2-2-P, CTQ2015-65816-R and PGC2018-093745-B-I00) is gratefully acknowledged. Moreover, this work was funded by the Xunta de Galicia (ED431D 2017/06, ED431E 2018/08 and GRC ED431C 2016/001) and the Junta de Castilla y León (Project VA124G18). All these research projects were partially supported by FEDER. H. M-C. and J. M. O-M. thank the Spanish Ministry of Education for their FPU

grant. Facilities provided by the Galician Supercomputing Centre (CESGA) are also acknowledged, as well as funding from the European Union (COST Actions CM1206 and MP1303).

References

[1] R. D. Rogers and K. R. Seddon, *Science*, 2003, **302**, 792–793.

[2] K. R. Seddon, *Nat. Mater.*, 2003, **2**, 363–365.

[3] N. V. Plechkova and K. R. Seddon, in *Ionic Liquids: "Designer" Solvents for Green Chemistry*, John Wiley & Sons, Inc., 2007, pp. 103–130.

[4] D. R. MacFarlane, M. Forsyth, P. C. Howlett, J. M. Pringle, J. Sun, G. Annat, W. Neil and E. I. Izgorodina, *Acc. Chem. Res.*, 2007, **40**, 1165–1173.

[5] M. Armand, F. Endres, D. R. MacFarlane, H. Ohno and B. Scrosati, *Nat. Mater.*, 2009, **8**, 621–629.

[6] X. Lu, G. Burrell, F. Separovic and C. Zhao, *J. Phys. Chem. B.*, 2012, **116**, 9160–9170.

[7] M. V. Fedorov and A. A. Kornyshev, *Chem. Rev.*, 2014, **114**, 2978–3036.

[8] M. C. Buzzeo, R. G. Evans and R. G. Compton, *Chem. Phys. Chem.*, 2004, **5**, 1106–1120.

[9] F. Endres and S. Z. E. Abedin, *Phys. Chem. Chem. Phys.*, 2006, **8**, 2101–2116.

[10] M. Galiński, A. Lewandowski and I. Stepniak, *Electrochim. Acta*, 2006, **51**, 5567–5580.

[11] H. Sakaebe and H. Matsumoto, *Electrochem. Commun.*, 2003, **5**, 594–598.

[12] B. García, S. Lavallée, G. Perron, C. Michot and M. Armand, *Electrochim. Acta*, 2004, **49**, 4583–4588.

[13] W. A. Henderson and S. Passerini, *Chem. Mater.*, 2004, **16**, 2881–2885.

[14] M. Diaw, A. Chagnes, B. Carré, P. Willmann and D. Lemordant, *J. Power Sources*, 2005, **146**, 682–684.

[15] Q. Zhou, W. A. Henderson, G. B. Appetecchi and S. Passerini, *J. Phys. Chem. C*, 2010, **114**, 6201–6204.

[16] S. Y. Lee, H. H. Yong, Y. J. Lee, S. K. Kim and S. Ahn, *Green Chem.*, 2005, **109**, 13663–13667.

[17] I. Nicotera, C. Oliviero, W. A. Henderson, G. B. Appetecchi and S. Passerini, *J. Phys. Chem. B*, 2005, **109**, 22814–22819.

[18] M. Castriota, T. Caruso, R. G. Agostino, E. Cazzanelli, W. A. Henderson and S. Passerini, *J. Phys. Chem. A*, 2005, **109**, 92–96.

[19] J. Lassègues, J. Grondin and D. Talaga, *Phys. Chem. Chem. Phys.*, 2006, **8**, 5629–5632.

[20] E. Markevich, V. Baranchugov and D. Aurbach, *Electrochem. Commun.*, 2006, **8**, 1331–1334.

[21] J. Xu, J. Yang, Y. NuLi, J. Wang and Z. Zhang, *J. Power Sources*, 2006, **160**, 621–626.

[22] S. Seki, Y. Kobayashi, H. Miyashiro, Y. Ohno, A. Usami, Y. Mita, N. Kihira, M. Watanabe and N. Terada, *J. Phys. Chem. B*, 2006, **110**, 10228–10230.

[23] M. Egashira, H. Todo, N. Yoshimoto, M. Morita and J. Yamaki, *J. Power Sources*, 2007, **174**, 560–564.

[24] Y. Saito, T. Umecky, J. Niwa, T. Sakai and S. Maeda, *J. Phys. Chem. B*, 2007, **111**, 11794–11802.

[25] V. Borgel, E. Markevich, D. Aurbach, G. Semrau and M. Schmidt, *J. Power Sources*, 2009, **189**, 331–336.

[26] J. Lassègues, J. Grondin, C. Aupetit and P. Johansson, *J. Phys. Chem. A*, 2009, **113**, 305–314.

[27] B. G. Nicolau, A. Sturlaugson, K. Fruchey, M. C. C. Ribeiro and M. D. Fayer, *J. Phys. Chem. B*, 2010, **114**, 8350–8356.

[28] Q. Zhou, K. Fitzgerald, P. D. Boyle and W. A. Henderson, *Chem. Mater.*, 2010, **22**, 1203–1208.

[29] H. Yoon, G. Lane, Y. Shekibi, P. Howlett, M. Forsyth, A. Best and D. MacFarlane, *Energy Environ. Sci.*, 2013, **6**, 979–986.

[30] F. Castiglione, A. Famulari, G. Raos, S. V. Meille, A. Mele, G. B. Appetecchi and S. Passerini, *J. Phys. Chem. B*, 2014, **118**, 13679–13688.

[31] L. Aguilera, J. Völkner, A. Labrador and A. Matic, *Phys. Chem. Chem. Phys.*, 2015, **17**, 27082–27087.

[32] A. Lahiri, G. Li, M. Olschewski and F. Endres, *ACS Appl. Mater. Interfaces*, 2016, **8**, 34143–34150.

[33] S. Menne, J. Pires, M. Anouti and A. Balducci, *Electrochem. Commun.*, 2013, **31**, 39–41.

[34] T. Vogl, C. Vaalma, D. Buchholz, M. Secchiaroli, R. Marassi, S. Passerini and A. Balducci, *J. Mater. Chem. A*, 2016, **4**, 10472–10478.

[35] G. T. Cheek, W. E. O'Grady, S. Z. El Abedin, E. M. Moustafa and F. Endres, *J. Electrochem. Soc.*, 2008, **155**, D91–D95.

[36] G. A. Giffin, A. Moretti, S. Jeong and S. Passerini, *J. Phys. Chem. C*, 2014, **118**, 9966–9973.

[37] G. Vardar, A. E. S. Sleightholme, J. Naruse, H. Hiramatsu, D. J. Siegel and C. W. Monroe, *ACS Appl. Mater. Interfaces.*, 2014, **6**, 18033–18039.

[38] S. Saha, T. Taguchi, N. Tachikawa, K. Yoshii and Y. Katayama, *Electrochim. Acta*, 2015, **183**, 42 – 48.

[39] J. Sun, R. C. Remsing, Y. Zhang, Z. Sun, A. Ruzsinszky, H. Peng, Z. Yang, A. Paul, U. Waghmare, X. Wu *et al.*, *arXiv preprint arXiv:1511.01089*, 2015.

[40] M.-C. Lin, M. Gong, B. Lu, Y. Wu, D.-Y. Wang, M. Guan, M. Angell, C. Chen, J. Yang, B.-J. Hwang *et al.*, *Nature*, 2015, **520**, 324.

[41] V. Gómez-González, B. Docampo-Álvarez, T. Méndez-Morales, O. Cabeza, V. B. Ivaništšev, M. V. Fedorov, L. J. Gallego and L. M. Varela, *Phys. Chem. Chem. Phys.*, 2017, **19**, 846–853.

[42] V. Gómez-González, B. Docampo-Álvarez, J. M. Otero-Mato, O. Cabeza, L. J. Gallego and L. M. Varela, *Phys. Chem. Chem. Phys.*, 2018, **20**, 12767–12776.

[43] V. Gómez-González, B. Docampo-Álvarez, H. Montes-Campos, J. C. Otero, E. López Lago, O. Cabeza, L. J. Gallego and L. M. Varela, *Phys. Chem. Chem. Phys.*, 2018, **20**, 19071–19081.

[44] M. V. Fedorov and R. M. Lynden-Bell, *Phys. Chem. Chem. Phys*, 2012, **14**, 2552–2556.

[45] S. Jo, S.-W. Park, C. Noh and Y. Jung, *Electrochim. Acta*, 2018, **284**, 577–586.

[46] T. Méndez-Morales, J. Carrete, S. Bouzón-Capelo, M. Pérez-Rodríguez, O. Cabeza, L. J. Gallego and L. M. Varela, *J. Phys. Chem. B*, 2013, **117**, 3207–3220.

[47] T. Méndez-Morales, J. Carrete, O. Cabeza, O. Russina, A. Triolo, L. J. Gallego and L. M. Varela, *J. Phys. Chem. B*, 2014, **118**, 761–770.

[48] Y. Zhang, A. Rubio and G. Le Lay, *J. Phys. D: Appl. Phys.*, 2017, **50**, 053004.

[49] I. Boustani, *Surf. Sci.*, 1997, **370**, 355–363.

[50] A. J. Mannix, X.-F. Zhou, B. Kiraly, J. D. Wood, D. Alducin, B. D. Myers, X. Liu, B. L. Fisher, U. Santiago, J. R. Guest *et al.*, *Science*, 2015, **350**, 1513–1516.

[51] A. J. Mannix, Z. Zhang, N. P. Guisinger, B. I. Yakobson and M. C. Hersam, *Nat. nanotechnol.*, 2018, **13**, 444.

[52] H. Tang and S. Ismail-Beigi, *Phys. Rev. Lett.*, 2007, **99**, 115501.

[53] X.-F. Zhou, X. Dong, A. R. Oganov, Q. Zhu, Y. Tian and H.-T. Wang, *Phys. Rev. Lett.*, 2014, **112**, 085502.

[54] J. Carrete, W. Li, L. Lindsay, D. A. Broido, L. J. Gallego and N. Mingo, *Mater. Res. Lett.*, 2016, **4**, 204–211.

[55] A. García-Fuente, J. Carrete, A. Vega and L. Gallego, *Phys. Chem. Chem. Phys.*, 2017, **19**, 1054–1061.

[56] S. Er, G. A. de Wijs and G. Brocks, *J. Phys. Chem. C*, 2009, **113**, 18962–18967.

[57] L. Li, H. Zhang and X. Cheng, *Comp. Mater. Sci.*, 2017, **137**, 119–124.

[58] A. Lebon, R. Aguilera-del Toro, L. Gallego and A. Vega, *Int. J. Hydrogen Energ.*, 2019, **44**, 1021–1033.

[59] X. Zhang, J. Hu, Y. Cheng, H. Y. Yang, Y. Yao and S. A. Yang, *Nanoscale*, 2016, **8**, 15340–15347.

[60] G. Kresse and J. Furthmüller, *Phys. Rev. B*, 1993, **47**, R558.

[61] G. Kresse and J. Furthmüller, *Phys. Rev. B*, 1996, **54**, 11169.

[62] G. Kresse and J. Furthmüller, *Comput. Mater. Sci.*, 1996, **6**, 15–50.

[63] G. Kresse and D. Joubert, *Phys. Rev. B*, 1999, **59**, 1758.

[64] G. Henkelman, A. Arnaldsson and H. Jónsson, *Comp. Mater. Sci.*, 2006, **36**, 354–360.

[65] E. Sanville, S. D. Kenny, R. Smith and G. Henkelman, *J. Comput. Chem.*, 2007, **28**, 899–908.

[66] W. Tang, E. Sanville and G. Henkelman, *J. Phys. Condens. Matter*, 2009, **21**, 084204–084210.

[67] M. Yu and D. R. Trinkle, *J. Chem. Phys.*, 2011, **134**, 064111–064118.

[68] B. Hess, C. Kutzner, D. V. D. Spoel and E. Lindahl, *J. Chem. Theory Comput.*, 2008, **4**, 435–447.

[69] M. J. Abraham, T. Murtola, R. Schulz, S. Páll, J. C. Smith, B. Hess and E. Lindahl, *SoftwareX*, 2015, **1**, 19–25.

[70] W. L. Jorgensen, *J. Phys. Chem.*, 1986, **90**, 1276–1284.

[71] V. Gómez-González, B. Docampo-Álvarez, O. Cabeza, M. V. Fedorov, R. M. Lynden-Bell, L. J. Gallego and L. M. Varela, *J. Chem. Phys.*, 2015, **143**, 124507.

[72] K. Mecke, *Phys. Rev. E*, 1996, **53**, 4794.

[73] N. Otsu, *IEEE Trans. Syst., Man, Cybern. B*, 1979, **9**, 62–66.

[74] A. Lopez-Bezanilla and P. B. Littlewood, *Phys. Rev. B*, 2016, **93**, 241405.

[75] C. E. Shannon, *Bell Labs Tech. J*, 1948, **27**, 379–423.

[76] T. Yan, C. J. Burnham, M. G. D. Pópolo and G. A. Voth, *J. Phys. Chem. B*, 2004, **108**, 11877–11881.

[77] M. Salanne, *Physical Chemistry Chemical Physics*, 2015, **17**, 14270–14279.

[78] V. Lesch, H. Montes-Campos, T. Méndez-Morales, L. J. Gallego, A. Heuer, C. Schröder and L. M. Varela, *The Journal of Chemical Physics*, 2016, **145**, 204507.

[79] S. Gabl, C. Schröder and O. Steinhauser, *J. Chem. Phys.*, 2012, **137**, 094501.

[80] G. Kikugawa, S. Ando, J. Suzuki, Y. Naruke, T. Nakano and T. Ohara, *J. Chem. Phys.*, 2015, **142**, 024503.

[81] A. Botan, V. Marry and B. Rotenberg, *Mol. Phys.*, 2015, **113**, 2674–2679.

[82] P. Simonnin, B. Noetinger, C. Nieto-Draghi, V. Marry and B. Rotenberg, *J. Chem. Theory Comput.*, 2017, **13**, 2881–2889.